Electronic Supplementary Material (ESI) for Catalysis Science & Technology.

Supporting Information for

Squalene-Polyethyleneimine-Dynamic Constitutional Frameworks Enhancing Enzymatic Activity of Carbonic Anhydrase

Dan-Dan Su,[a, b] Karim Aissou,[a] Yan Zhang,[c] Virginie Gervais,[d] Sebastien Ulrich,*[b] and Mihail Barboiu*[a]

a. Institut Européen des Membranes, Adaptive Supramolecular Nanosystems Group, University of Montpellier, ENSCM-CNRS, Place E. Bataillon CC047, Montpellier, F-34095, France. E-mail: mihail-dumitru.barboiu@umontpellier.fr.
b. Institut des Biomolécules Max Mousseron (IBMM), CNRS, Université de Montpellier, ENSCM, Montpellier, France. E-mail: sebastien.ulrich@cnrs.fr.
c. Key Laboratory of Carbohydrate Chemistry and Biotechnology, Ministry of Education, School of Pharmaceutical Sciences, Jiangnan University, 1800 Lihu Avenue, Wuxi, 214122, P.R. China.
d. Université Paris-Saclay, CEA, CNRS, Institute for Integrative Biology of the Cell (I2BC), 91198, Gif-sur-Yvette, France.

1. Materials and Methods

All reagents were obtained from Sigma Aldrich and were used without further purification. ^{1}H-NMR spectra were recorded on an ARX 400 MHz Bruker spectrometer in $CDCl_3$ and D_2O as an internal standard. Fluorescence spectra were obtained in a SAFAS Xenius spectrofluorometer. UV-vis spectra were recorded on a SAFAS UV mc spectrophotometer. Dynamic light scattering experiments were carried out on Zetasizer Nano (Malvern). Transmission Electron Microscopy-TEM images were obtained by using a JEM 1400+ electron microscopy: 10 µL of the sample was dropped on a carbon coated copper grid, then the sample was blotted with filter paper and dried at room temperature. The sample was observed at a 120 kV acceleration voltage at 25°C. Atomic force microscopy (AFM Nano-Observer, CS Instruments) was used in tapping mode to characterize the surface morphology of all samples. Silicon cantilevers (PPP-NCH, Nanosensors), with a typical tip radius of ~5 nm, were used. The resonance frequency of the cantilevers was about 235 kHz.

2. Synthesis of 1,1',2-Tris-nor-squlaene aldehyde

Synthesis of 1,1',2-Tris-nor-squlaene aldehyde was obtained through a 3-step reaction (**Scheme S1**).[1]

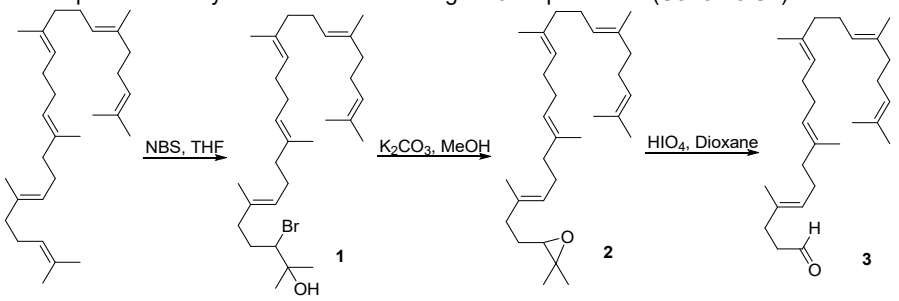

Scheme S1 Synthetic route of 1, 1', 2-Tris-nor-squalene aldehyde, **SQ-CHO**

Synthesis of 2-Hydroxy-3-bromosqualene (1): To a solution of squalene (4.290 g, 10.4 mmol) in tetrahydrofuran (30 mL), a small amount of water was added and then tetrahydrofuran drop-wise to obtain a clear solution. N-bromosuccinimide (2.231 g, 12.5 mmol) was added during 30 minutes and then the reaction mixture was stirred for three hours. After evaporation in vacuo, the obtained oil was added to brine solution (100 mL) and the product was extracted with ethyl acetate (150 mL). The organic solution was dried over anhydrous Na_2SO_4 and the solvent was removed in vacuo. The crude was purified by flash chromatography to acquire 2-Hydroxy-3-bromosqualene. Yield: 27.2%. ^{1}H-NMR ($CDCl_3$, 400 MHz): δ=5.20-5.14 (m, 5H); 3.98-3.96 (dd, 1H); 2.35-2.32 (m, 1H); 2.16-1.99 (m, 18H); 1.81-1.79 (m, 1H); 1.67 (s, 3H); 1.60 (bs, 15H); 1.34 (s, 3H); 1.32 (s, 3H).

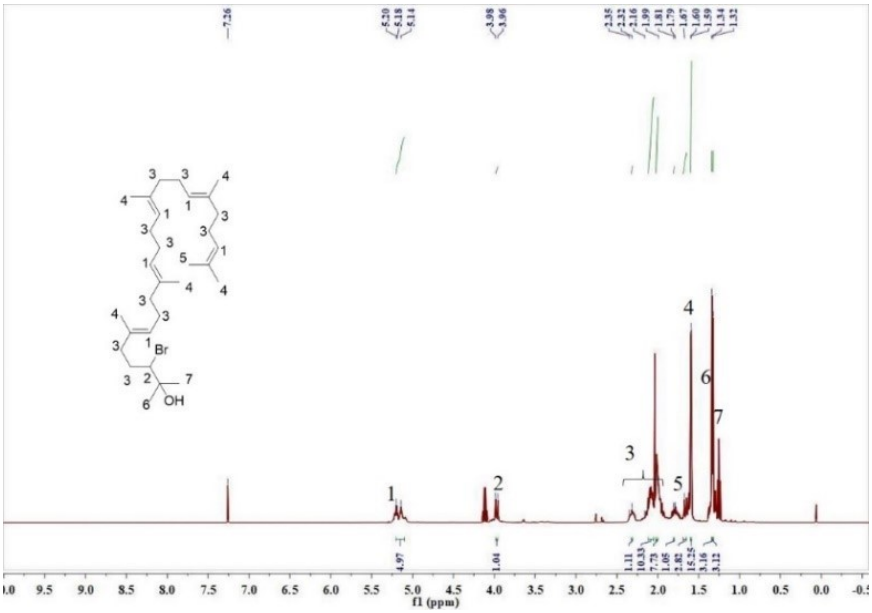

Figure S1 ^{1}H NMR spectrum of 2-Hydroxy-3-bromosqualene in $CDCl_3$.

Synthesis of 2, 3-oxidosqualene (2). To a solution of 2-Hydroxy-3-bromosqualene (1.652 g, 3.2 mmol) in methanol (60 mL), K_2CO_3 (0.898 g, 6.5 mmol) was added and the mixture was stirred for 2 h at room temperature. Then the solution was concentrated in vacuo. Water (100 mL) was added and extracted with ethyl acetate (120 mL). The organic solution was dried over anhydrous Na_2SO_4 and 2,3-oxidosqualene was obtained after removal of the solvent. Yield: 73.3%. ^{1}H-NMR ($CDCl_3$, 400 MHz): δ=5.16-5.14 (m, 5H); 2.70 (t, 1H); 2.15-2.00 (m, 20H); 1.68 (s, 3H); 1.61 (s, 3H); 1.60 (bs, 12H); 1.30 (s, 3H); 1.25 (bs, 3H).

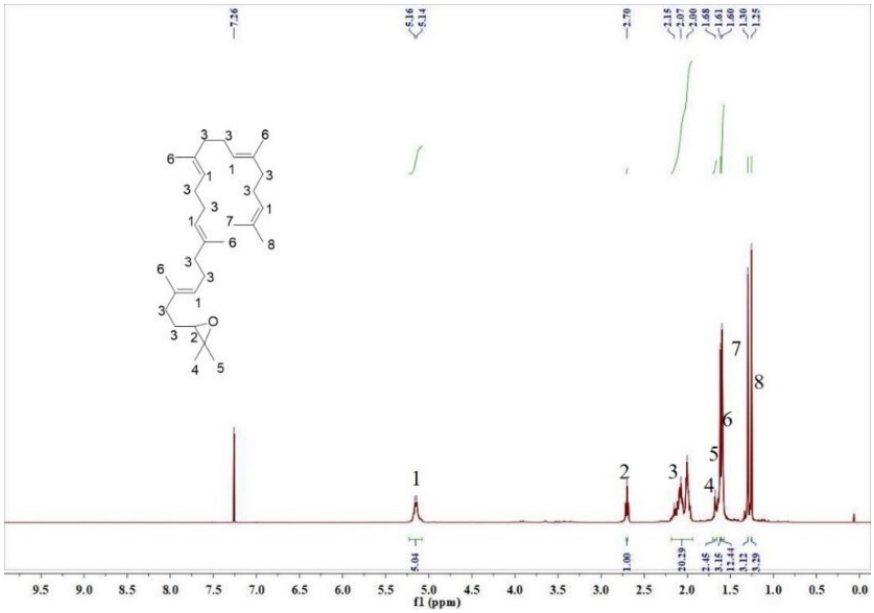

Figure S2 ^{1}H NMR spectrum of 2,3-oxidosqualene in $CDCl_3$.

Synthesis of 1,1',2-Tris-nor-squalene aldehyde (3): To a solution of periodic acid (1.379 g, 6.0 mmol) in 5 mL of water, a solution of 2,3-oxidosqualene (1.434 g, 3.4 mmol) in 12 mL of dioxane was added. The reaction mixture was stirred for 2 h at room temperature. Water (120 mL) was added and extracted with ethyl acetate (120 mL). The organic solution was washed with brine and water, then dried over anhydrous Na_2SO_4 and the solvent was removed to get 1,1',2-Tris-nor-squalene aldehyde. Yield: 81.1%. ^{1}H-NMR ($CDCl_3$, 400 MHz): δ=9.74 (s, 1H); 5.16-5.12 (m, 5H); 2.50 (t, 2H); 2.31 (t, 2H); 2.13-1.97 (m, 16H); 1.67 (s, 3H); 1.55 (bs, 15H).

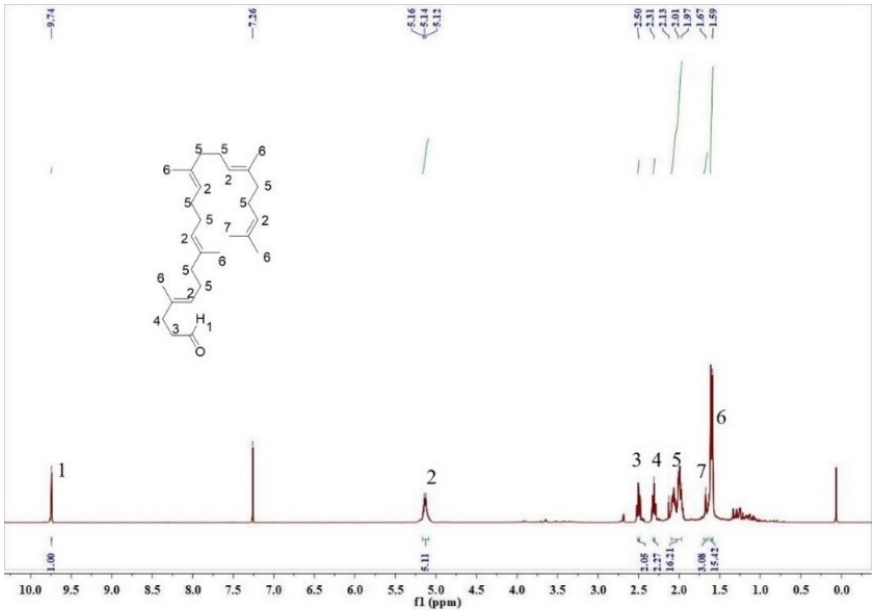

Figure S3 ^{1}H NMR spectrum of 1, 1', 2-Tris-nor-squalene aldehyde in $CDCl_3$.

3. Synthesis of DCFs

Preparation of PEGylated squalene (SQ-PEG1500): Poly(ethylene glycol) diamine 1500 (445 mg, 0.297 mmol, 1.1 eq) and 1,1',2-Tris-nor-squalene aldehyde (SQ-CHO) (104 mg, 0.27 mmol, 1 eq) were dissolved in acetonitrile (12.5 mL) and stirred for 24h at room temperature. The products were verified through NMR. The solution was stocked and used directly for the next step. ^{1}H-NMR (400 MHz, $CDCl_3$, TMS): δ=7.63 (t, 1H), 5.19-5.09 (m, 5H), 3.65 (m, 182H), 3.08-3.05 (m, 2H), 2.06-1.98 (m, 20H), 1.67-1.59 (m, 18H).[2]

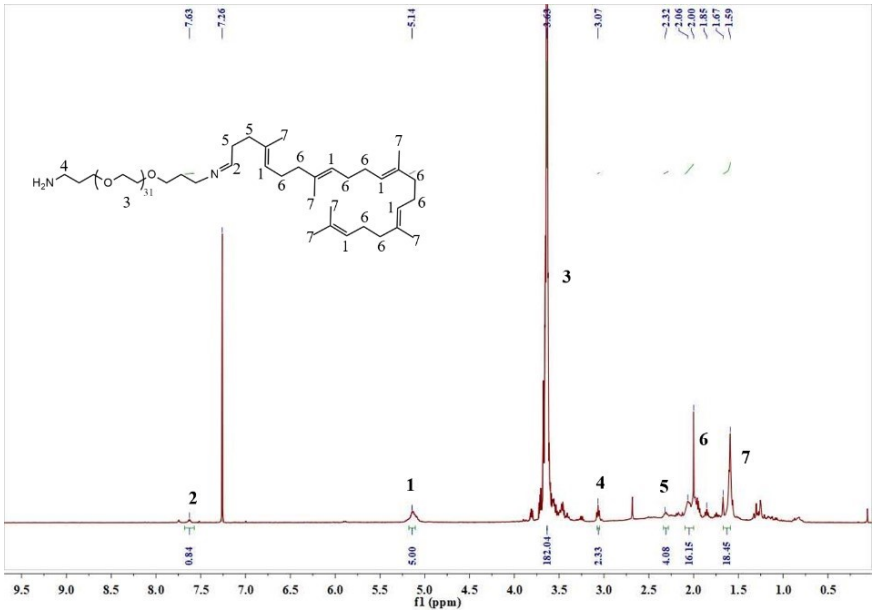

Figure S4 ^{1}H NMR spectrum of SQ-PEG1500 in $CDCl_3$.

Preparation of the intermediary units: To a solution of SQ-PEG1500 (0.27 mmol, 1 eq), a solution of 1,3,5-benzenetrialdehyde (43.4 mg, 0.27 mmol, 1 eq) in 10 mL of acetonitrile was added, reaction mixture was stirred at room temperature. Solvent was monitored through ^{1}H NMR until the equilibrium was reached. The solvent was removed and milli-Q H_2O was added to prepare a 10 mM stock solution for the next step.

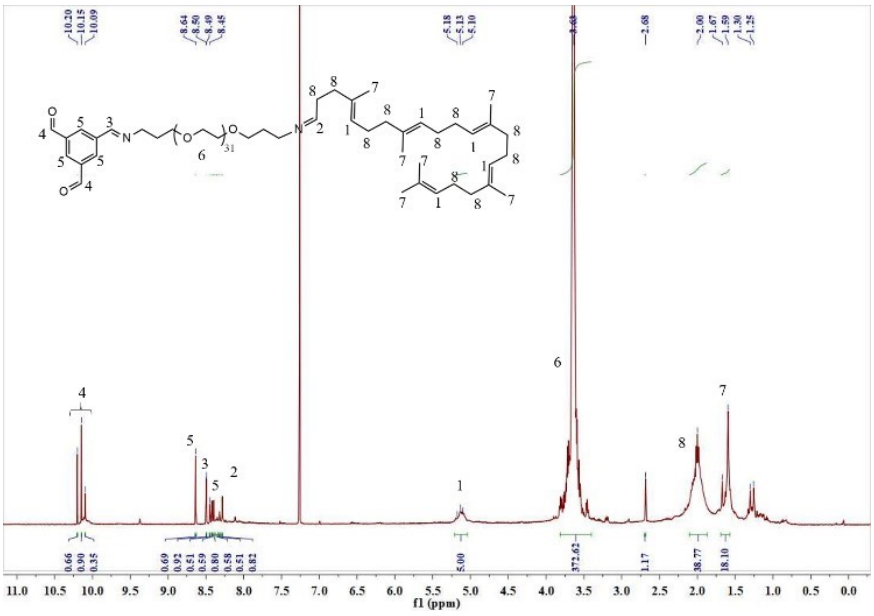

Figure S5 ^{1}H NMR spectrum of SQ-PEG1500-BTA in $CDCl_3$.

Synthesis of DCFs: Positively-charged Polyethyleneimine 800, bPEI800 (1 mL of 20 mM aqueous solution, 2 eq), Pentaethylene-hexamine, PEH (1 mL of 20 mM aqueous solution, 2 eq), Tris-2-aminoethylamine, TAA (1 mL of 20 mM aqueous solution, 2 eq) were added to the above intermediary units aqueous solution (1 mL, 10 mM, 1 eq) separately to obtain corresponding stock DCFs aqueous solution (5 mM). Solvent was monitored through ^{1}H NMR until the equilibrium was reached.

4. Fluorescence Studies

CA solution was prepared by adding 2.5 mg of CA powder in to 1 mL of PBS buffer solution. 3 µL of bCA was added to 3 mL of PBS buffer solution in a 3 mL quartz cuvette. Then the initial fluorescence of bCA was recorded at 280 nm as excitation wavelength, and from 290 nm to 400 nm as emission wavelength, at 500 PM. Then the intensity change was measured with the increasing addition of DCFs into the same cuvette (**Figure S6**). The association constant (K_a) was calculated by using Stern-Volmer relation ($I_0/I=1+K_a[P]$). I_0 is the initial fluorescence intensity of bCA; I is the intensity of bCA with the presence of DCFs at the highest fluorescence intensity at 343 nm. [P] is the concentration of added DCFs/monomers. PBS buffer solution (pH 7.4, 1 L) was prepared as following: NaCl 8 g, KCl 0.2 g, Na_2HPO_4 1.42 g, KH_2PO_4 0.27 g.

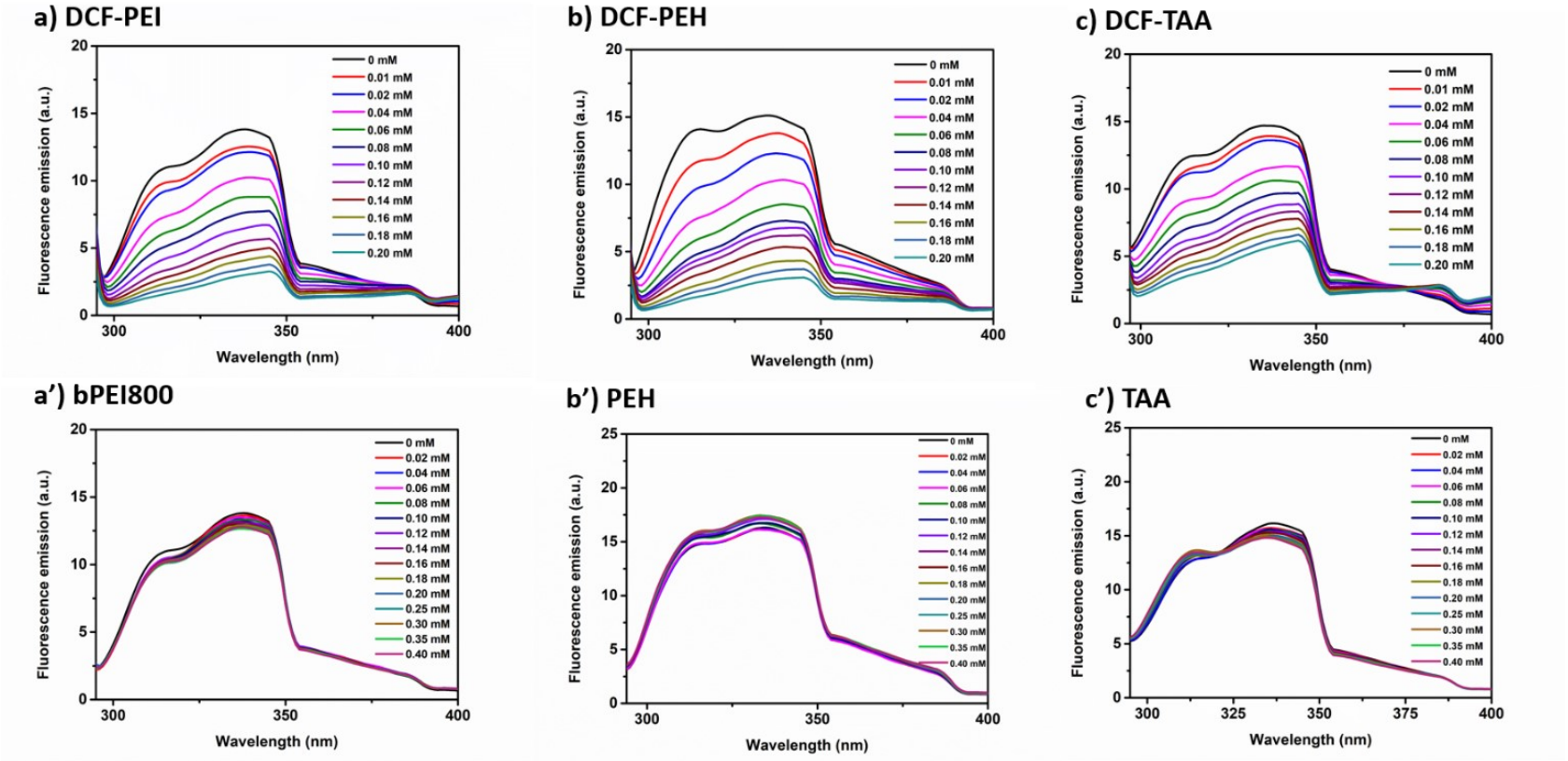

Figure S6 Fluorescence quenching of CA upon addition of increasing amount of a) **DCF-PEI**; a') **bPEI800**; b) **DCF-PEH**; b') **PEH**; c) **DCF-TAA**; c') **TAA** (The final concentration of monomers was varied from 0.02 mM to 0.40 mM, then the final concentration of DCFs was varied from 0.01 mM to 0.20 mM since they contained 2 eq. of monomers)

5. Isothermal titration calorimetry (ITC)

Experiments were performed at 25°C on a PEAK-ITC microcalorimeter (MicroCal Inc., Malvern Panalyticals). A first injection of 0.4 ul, which was not taken into account for the fitting, was followed by 20 injections of 2 ul of spacing180 s. The enzyme was resuspended in a PBS buffer. The thermostatic cell was filled with a solution of bCA enzyme (15-20 μM) and the syringe was loaded with ligand solution (200-250 μM). Control experiments were systematically carried out, in which the ligand solution was added to the buffer-containing cell. Reverse calorimetric titrations were also performed as controls (not shown), where bCA (500 μM) was used to titrate ligand solution present in the measurement cell (25-50 μM). Data were analyzed using the MicroCal Origin software provided by the manufacturer.

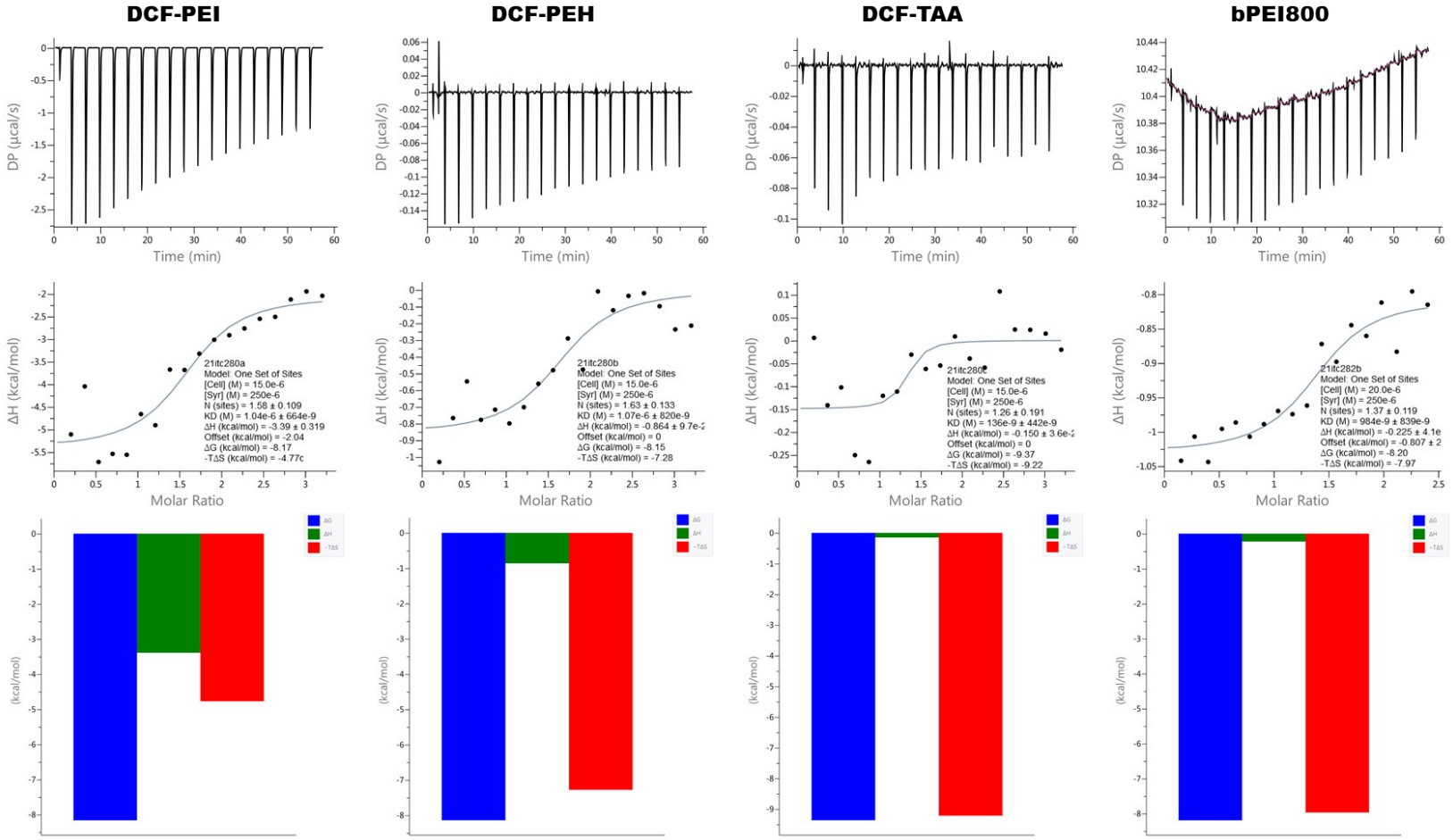

Figure S7 Binding of **DCF-PEI**, **DCF-PEH**, **DCF-TAA**, and **bPEI800** to bCA studied by ITC: binding isotherms (top), integrated individual heat flow signals as function of molar raction (middle), and histograms summarizing ΔG, ΔH, and -TΔS values (bottom).

6. Atomic Force Microscopy

Atomic Force Microscopy AFM images were recorded for the mixture of bCA with **DCF-PEI**, **DCF-PEH** and **DCF-TAA**. Prior AFM measurements, a DCF droplet was deposited on silicon substrate cleaned with acetone then was evaporated at ambient condition for 12 hours. The concentration of all samples was fixed at 30 µg/mL. The images of **DCF-PEH** with bCA and **DCF-TAA** with bCA present spherically-shaped particles with the size distributions of less than 200 nm. Free enzyme bCA may aggregate in aqueous solution due to hydrophobic interactions, which have been observed by analyzing HPLC traces.[3]

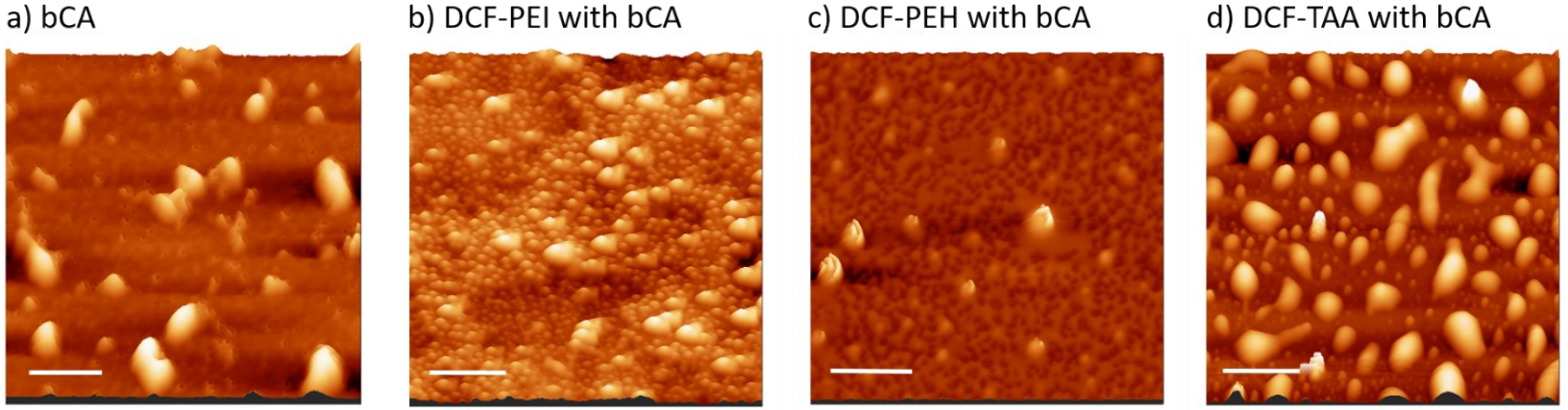

Figure S8 AFM images of **DCFs-bCA**: a) **bCA**. (2×2 µm) Scale bar: 400 nm; b) **DCF-PEI** with bCA. (5×5 µm) Scale bar: 1.0 µm; c) **DCF-PEH** with bCA. (5×5 µm) Scale bar: 1.0 µm and d) **DCF-TAA** with bCA. (5×5 µm) Scale bar: 1.0 µm.

7. UV-vis Studies

The hydrolysis reaction of *p*-nitrophenyl acetate was used to study the catalytic reactivity of bCA, as the formation of *p*-nitrophenol can be measured at 400 nm. 3.5 mM of *p*-NPA solution was prepared in CH_3CN. 300 µL *p*-NPA was added to a mixture of 30 µL bCA (0.1 mM) in 3 mL of PBS buffer (pH 7.4) and increasing amounts of DCFs/monomers in a quartz cuvette. The formation of *p*-NP over the first 4 min was monitored at 400 nm, using time-drive analysis method of UV-vis spectroscopy.

Calculation of synergistic activity.

Synergistic activity was calculated by the following equation:

$$N = \frac{A_1}{(A_0 + A_2)}$$

A_1: The absorbance measured with DCF or monomer with bCA at 4 min; A_0: The absorbance measured with CA alone at 4 min;
A_2: The absorbance of measured with DCF or monomer alone at 4 min.

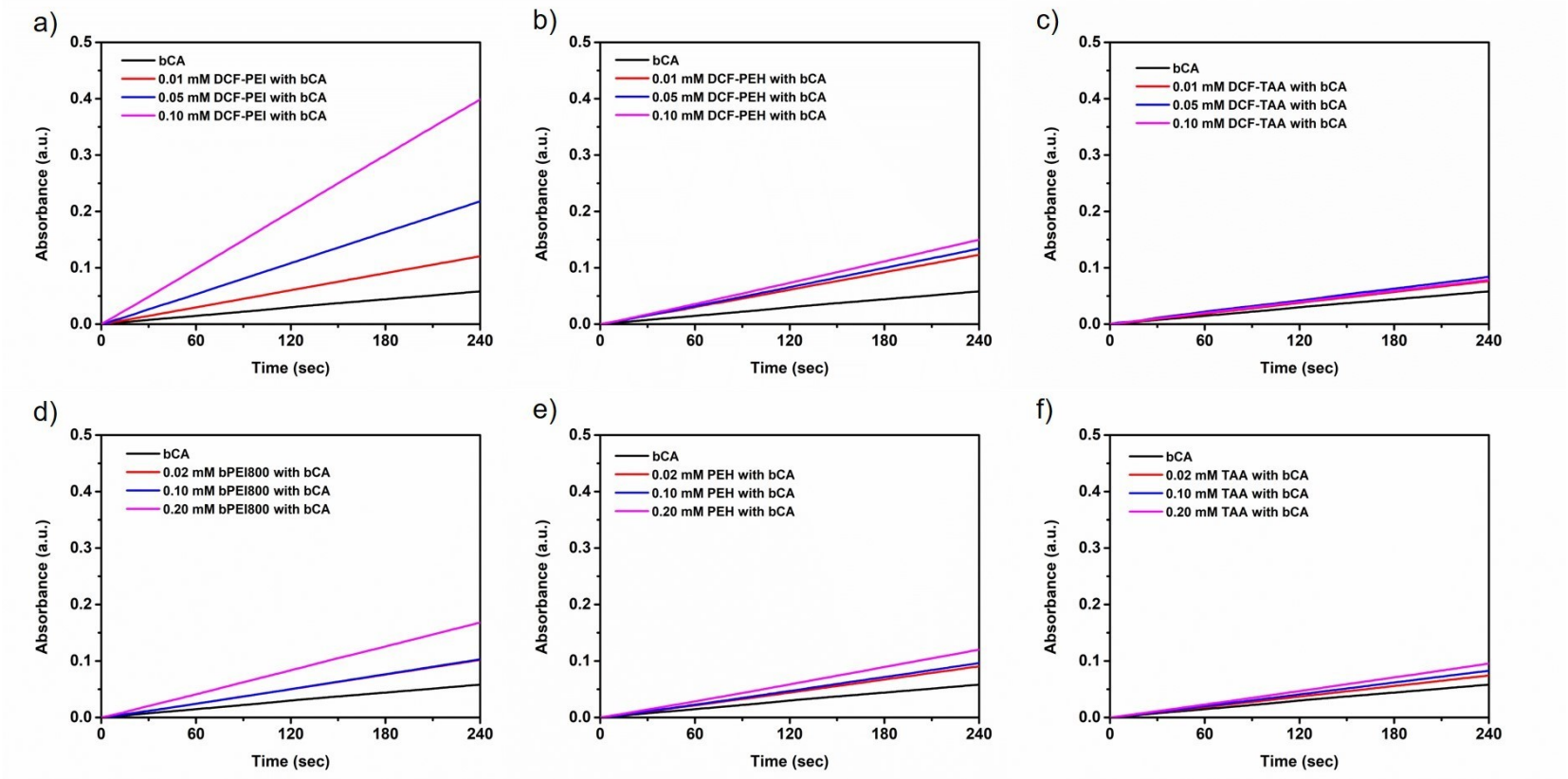

Figure S9 Enzymatic activity change of bCA on hydrolysis reaction of *p*-nitrophenyl acetate within 4 minutes with the increasing addition of a) **DCF-PEI**; a') **bPEI800**; b) **DCF-PEH**; b') **PEH**; c) **DCF-TAA**; c') **TAA**

The negative control experiments of hydrolysis reaction of *p*-nitrophenyl acetate without bCA were carried out to calculate the catalytic activity of DCFs/monomers.

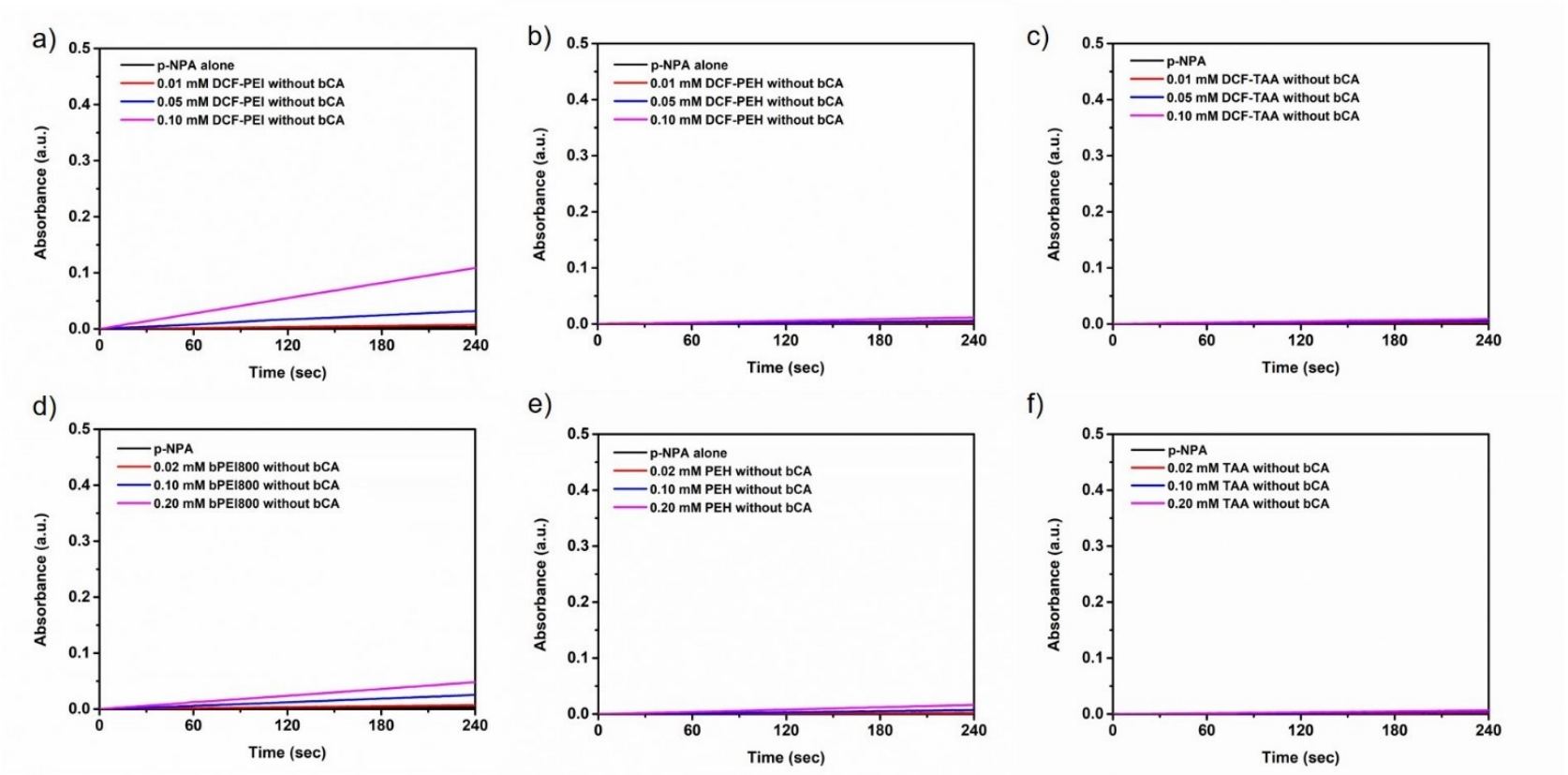

Figure S10 Control experiments of hydrolysis reaction of *p*-nitrophenyl acetate in the absence of bCA with the addition of a) **DCF-PEI**; a') **bPEI800**; b) **DCF-PEH**; b') **PEH**; c) **DCF-TAA**; c') **TAA**

Kinetic studies of CA upon addition of DCFs/monomers The kinetic parameters of the enzyme activation was evaluated through the same UV-vis kinetic method with the time-course analysis by changing the final concentration of *p*-NPA from 0.10 to 10 mM. The final concentration of DCFs/monomers were fixed to 0.2/0.4 mM respectively. 300 μL *p*-NPA was added to a mixture of 30 μL bCA (0.1 mM) in PBS buffer in a 3 mL quartz cuvette. The activity change of hydrolysis reaction with bCA are shown below.

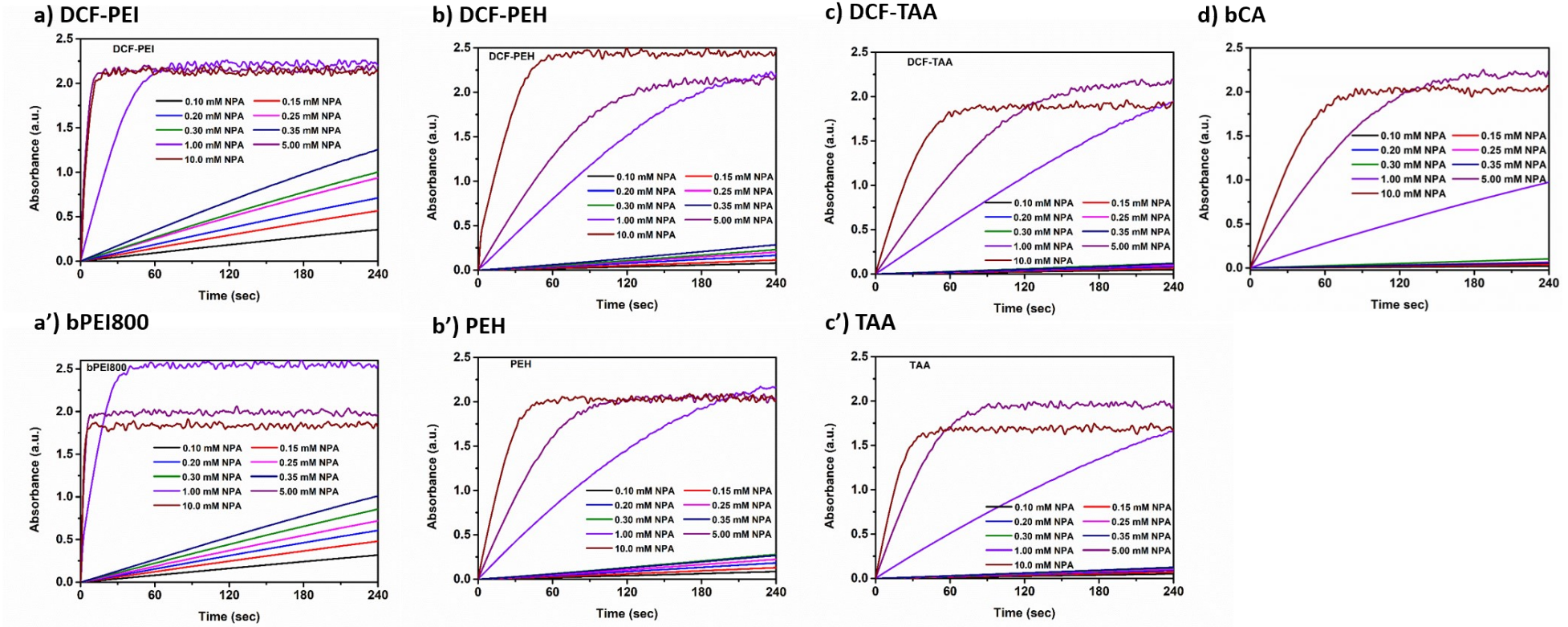

Figure S11 Activity change of bCA on hydrolysis reaction of different concentration of *p*-nitrophenyl acetate within 4 minutes with the increasing addition of a) **DCF-PEI**; a') **bPEI800**; b) **DCF-PEH**; b') **PEH**; c) **DCF-TAA**; c') **TAA**; d) **bCA**

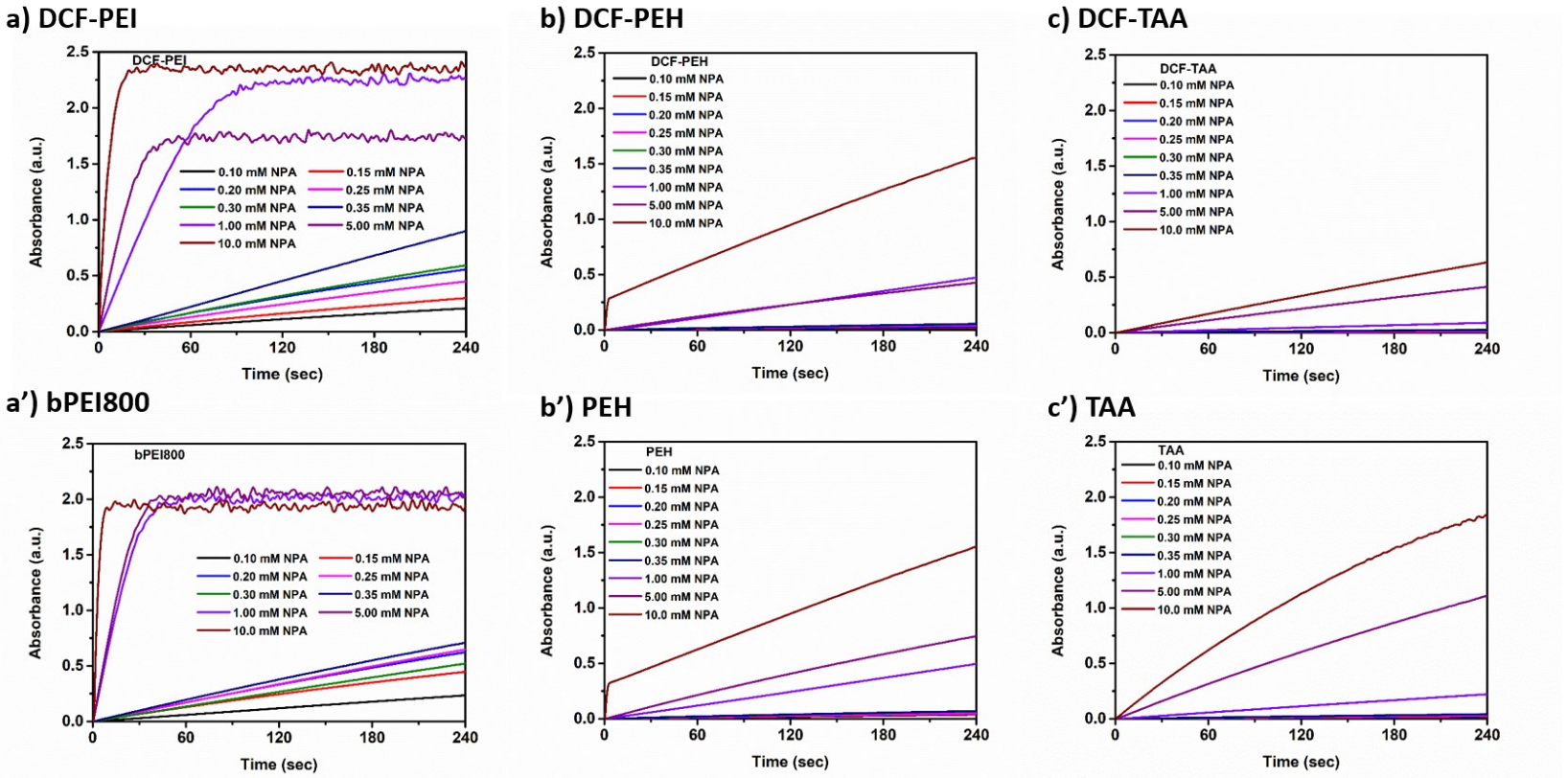

Figure S12 Control experiments of hydrolysis reaction of different concentration of *p*-nitrophenyl acetate in the absence of bCA with the addition of a) **DCF-PEI**; a') **bPEI800**; b) **DCF-PEH**; b') **PEH**; c) **DCF-TAA**; c') **TAA**

8. Calculation of K_m and V_{max}

K_m and V_{max} was determined according to the kinetic studies of CA upon addition of DCFs/monomers by using Michaelis Menten function in OriginPro 9.0, then k_{cat}/K_m was calculated by using $V_{max}/K_m[E]$ ([E] is the final concentration of enzyme : 0.001 mM). The initial rate was obtained by estimating the slopes which was fit the plots (Figure S11) using Linear Fit. The measurements of $\Delta A\ s^{-1}$ are converted to $M\ s^{-1}$ by using the molar extinction coefficient of *p*-nitrophenol ($17{,}000\ M^{-1}\ cm^{-1}$).[4] The assay of bCA itself is validated by the values of k_{cat}/K_m that we obtained which keeps the same order of magnitude as the previous values ($230.7\ M^{-1}\ s^{-1}$) reported in literature.[5,6]

Table S1 K_m, V_{max} and k_{cat}/K_m values of all samples

Sample	K_m (mM)	V_{max} ($M\ s^{-1}$)	[E] (mM)	k_{cat} (s^{-1})	k_{cat}/K_m ($M^{-1}\ s^{-1}$)
DCF-PEI with bCA	2.08	1.54E-05	0.001	15.36	7396
DCF-PEH with bCA	4.20	3.79E-06	0.001	3.79	902
DCF-TAA with bCA	3.71	2.49E-06	0.001	2.49	672
bPEI800 with bCA	1.68	1.11E-05	0.001	11.12	6630
PEH with bCA	3.36	2.77E-06	0.001	2.77	826
TAA with bCA	3.31	3.24E-06	0.001	3.24	978
bCA	3.13	1.58E-06	0.001	1.58	504

9. Calculation of the rate constant in the absence of bCA

With regard to the kinetic study in the absence of bCA (**Figure S12 and Figure S13**), the increasing absorbance observed is most likely the result of a direct reaction of DCF/Monomers onto *p*-NPA. We therefore estimated the observed rate constant of this background non-catalytic reaction assuming a 2nd order rate constant that fit the following equations: v=k[Monomer][NPA] or v=k[DCF][NPA]. The maximum rate constants of **DCF-PEI** and **bPEI800** are calculated from the starting linear part. The final concentration of DCFs/monomers were fixed to 0.2/0.4 mM respectively. As shown in **Table S2**, the obtained k value is far less than the k_{cat} of DCF/Monomer with bCA, which means this reaction plays a secondary role in the present assay.

Table S2 The maximum reaction rate k of DCF/Monomer

DCF	k ($M^{-1}\ s^{-1}$)	Monomer	k ($M^{-1}\ s^{-1}$)
DCF-PEI	4.23	bPEI800	2.79
DCF-PEH	0.19	PEH	0.10
DCF-TAA	0.08	TAA	0.13

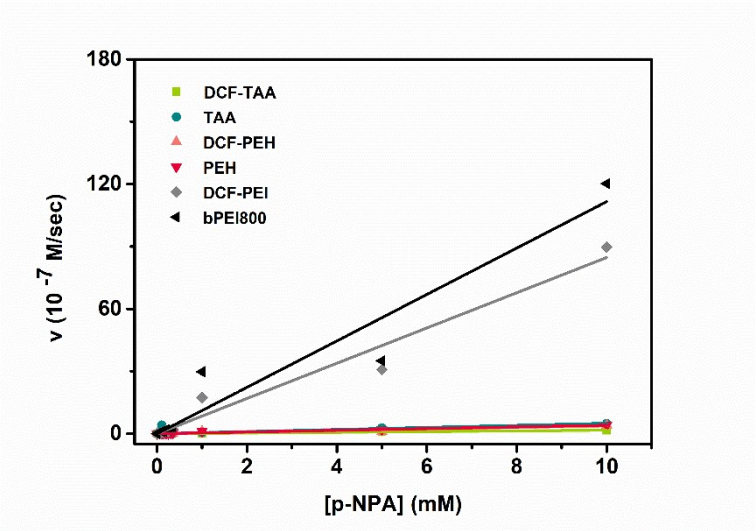

Figure S13 Estimation of rate constant of non-catalytic reaction for DCF and monomers in the absence of bCA

10. Enzyme activation at high temperature

In this part, the fluorescence emission of bCA was measured at a range of temperature from 20 to 80°C at pH 7.4, in order to test the binding behavior between **DCF-PEI** and enzyme at high temperature. The final concentration of **DCF-PEI** was controlled at 0.1 mM. From **Figure S14a**, the fluorescence absorption of bCA decreased with the improving of the surrounding temperature and it lost its activity about 55% at 80°C. As last the tryptophan fluorescence lost around 30% when it came to 20°C. As shown in **Figure S14b**, enzyme and **DCF-PEI** were mixed in the same cuvette for a few minutes and then the fluorescence emission was recorded, the complexes present 30% fluorescence loss also after high temperature damage. Then from **Figure S14c**, we can observe the similar trend as **Figure S14b**, with the addition of dynamer at 80°C, a sharp quench in fluorescence was shown.

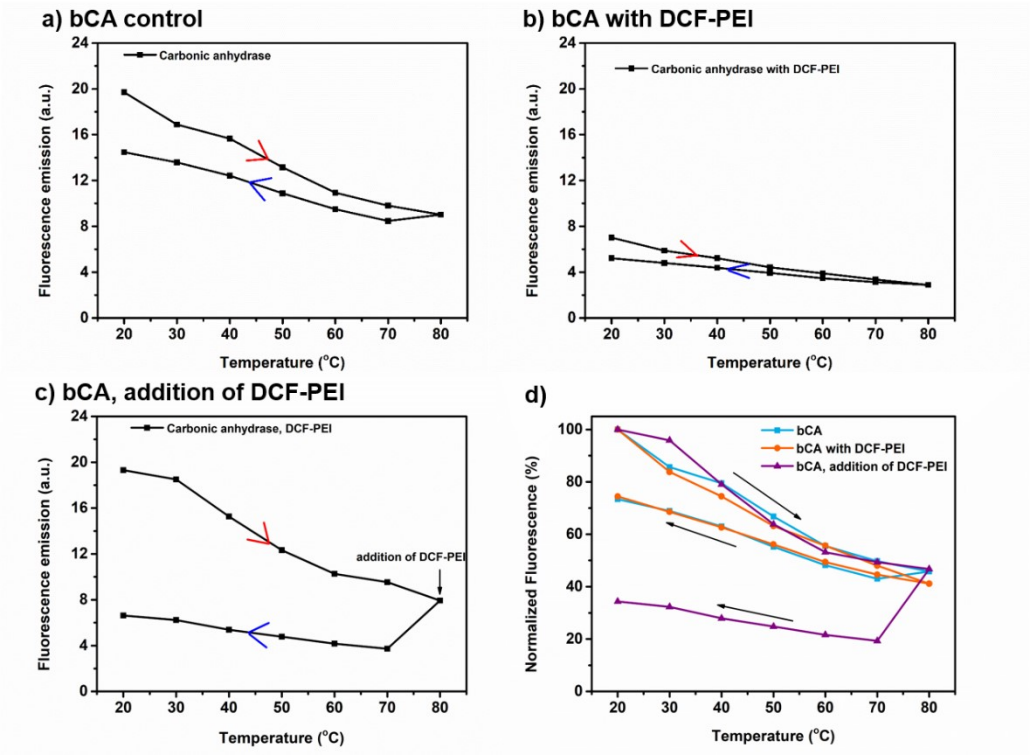

Figure S14 Fluorescence absorption of a) bCA, b) bCA with dynamer **DCF-PEI** with a range of temperature from 20°C to 80°C, c) bCA with the addition of dynamer **DCF-PEI** at 80°C, d) Normalized fluorescence absorption of three samples

The relative tryptophan fluorescence from bCA was measured at a range of temperature from 20 to 80°C at pH 7.4, in order to test the effect of **DCF-PEI** on enzyme tolerance to high temperature. The final concentration of **DCF-PEI** was 0.1 mM. As shown in **Figure S14d**, the fluorescence emission of bCA decreased with the rise in surrounding temperature. **DCF-PEI** didn't display any protection to bCA against denaturation at high temperature since it present the similar reducing trend.

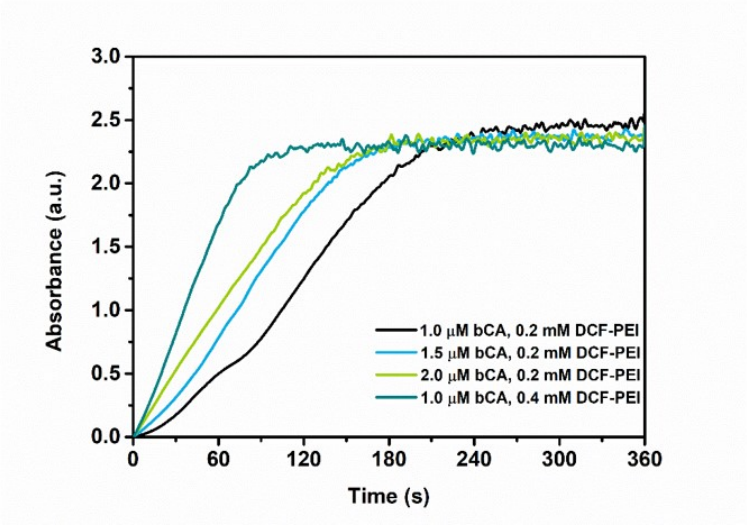

Figure S15 Activity change of **DCF-PEI** with different concentration of bCA at 80°C

As shown in **Figure S15**, the plateau was reached earlier with the increasing addition of bCA or **DCF-PEI**, which showed the remained enzyme activity at 80°C.

11. Dynamic light scattering

The particle size of all DCFs/monomers with enzyme were evaluated through dynamic light scattering as reported shown. The results showed that all DCFs present homogenous sizes, which **DCF-PEI** and **DCF-TAA** both showed a size of around 170 nm while the size of **DCF-PEH** was around 120 nm. With regard to the complexes formed by DCFs and enzyme, the presence of enzyme did not influence the size of DCFs (**Table S3**). The concentration of DCFs were fixed at 0.2 mM with or without enzyme.

The concentration of monomers was fixed at 0.4 mM. All samples present aggregated particle sizes. In addition, the size of **bPEI800**-bCA would be decreased to 336 nm with the decreasing concentration to 0.02 mM. The PDI values are very high, indicating highly polydisperse nanoparticles in the presence of PEI monomers. They are much more polydisperse than with the DCFs.

Table S3 Particle size by dynamic light scattering and partial observed structure by transmission electron microscopy of DCFs and dynamer/monomer-encapsulated bCA

Sample at 80°C	Size (nm)	PDI	Sample at 25°C	Size (nm)	PDI
DCF-PEI-bCA	1074.4±246.7	0.701±0.223	**DCF-PEI-bCA**	173.4±1.9	0.208±0.016
	Heterogeneous aggregation			Homogeneous nanoparticles	
bPEI800-bCA	Intertwined reticulated structure		**bPEI800 (0.4 mM)-bCA**	620.7±25.9	0.541±0.022
				Homogeneous aggregation	
Sample at 25°C	Size (nm)	PDI	Sample at 25°C	Size (nm)	PDI
DCF-PEH-bCA	124.1±0.1	0.284±0.001	**DCF-PEI**	173.5±0.2	0.204±0.022
				Homogeneous nanoparticles	
DCF-TAA-bCA	172.0±0.3	0.179±0.011	**DCF-PEH**	127.0±0.5	0.281±0.002
PEH-bCA	751.1±54.6	0.628±0.032	**DCF-TAA**	171.1±1.6	0.167±0.019
TAA-bCA	1078.5±246.8	0.670±0.111	**bPEI800 (0.02 mM)-bCA**	336.0±45.4	0.455±0.084

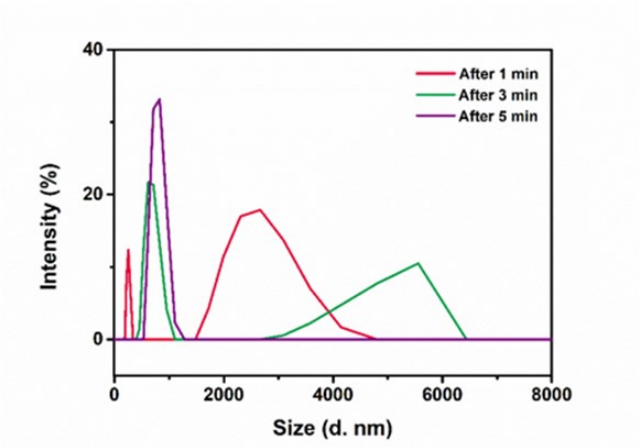

Figure S16 DLS distribution of dynamer-encapsulated enzyme at 80°C: **DCF-PEI** with bCA

The complex formed by **DCF-PEI** and bCA at 80°C was observed and as shown in **Figure S17**, it presents compact structure.

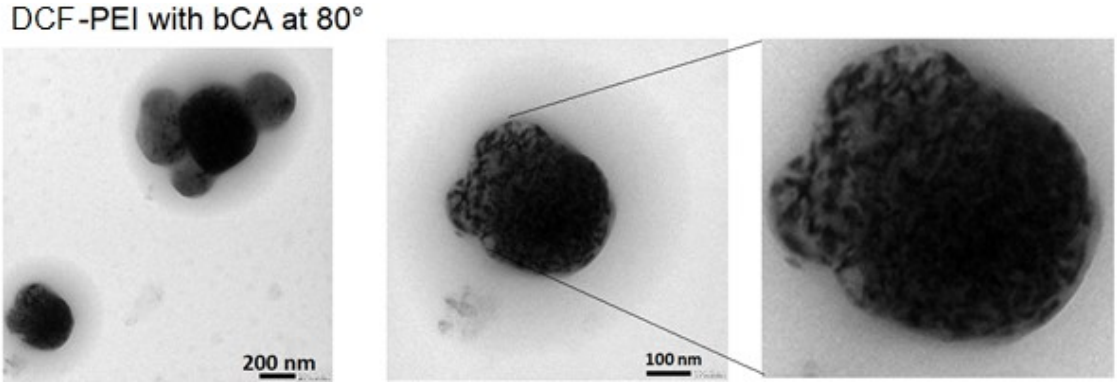

Figure S17 Representative TEM micrographs recorded from **DCF-PEI** with bCA after heating at 80°C

The complex formed by **bPEI800** and bCA at 80°C was also observed and as shown in **Figure S18,** it presents intertwined reticulated structure.

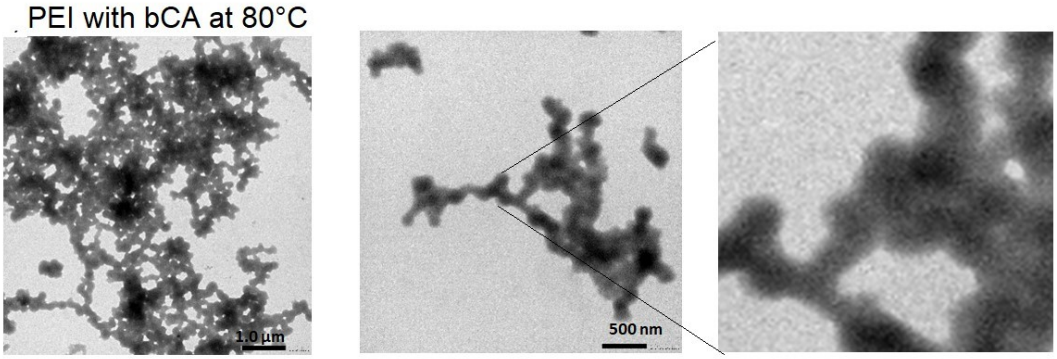

Figure S18 Representative TEM micrographs recorded from **bPEI800** with bCA after heating at 80°C

12. Characterization of hydrolysis reaction

The hydrolysis reaction of *p*-nitrophenyl acetate (**NPA**) with **PEI** was characterized by using NMR. The NMR peaks of **NPA** samples were shown in **Figure S18**, there is one signal around 1.87 ppm which belongs to acetic acid, which is distinguishable from the proton of acetylated CH_3- at 1.70-1.85 ppm.[7,8] And with the addition of **PEI**, the product **NP** was obtained as shown Peak 5 and Peak 4 in sample **NPA-PEI-1**. Apart from that, the peaks which are close to Peak 5 and Peak 4 probably attribute to the free **NP** encapsulated by **PEI**, since the chemical shifts of **NP** would move to high field due to the increased electron density on the benzene ring. Then with the increasing of **PEI**, all the **NPA** was consumed to **NP**. These results indicated that **NPA** was hydrolyzed with the involvement of **PEI** and no acetylation happened during the hydrolysis reaction of **NPA**.

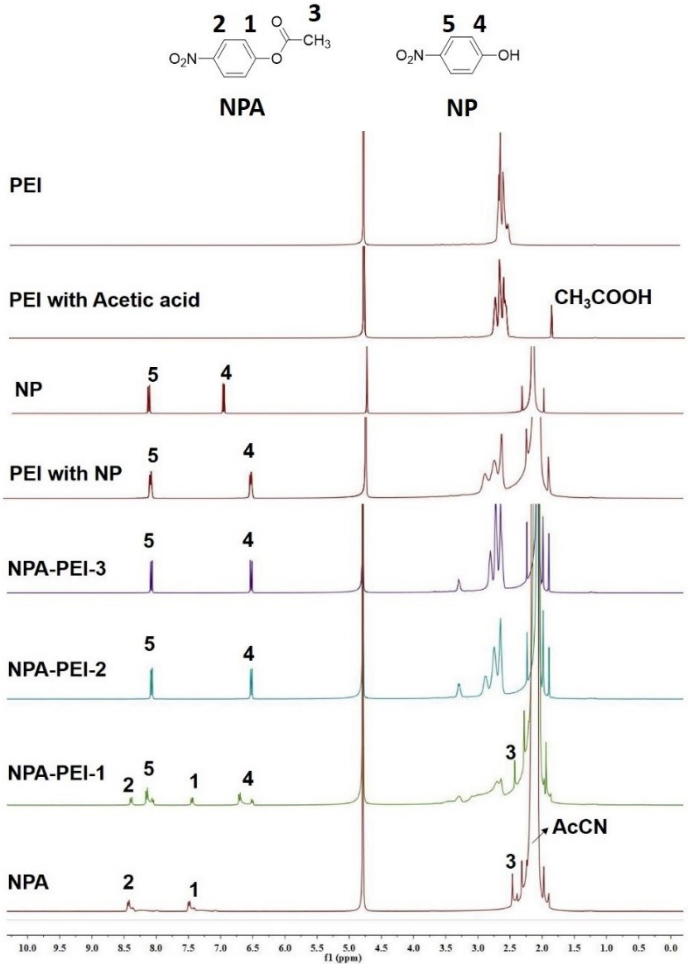

Figure S19 ^{1}H NMR of **NPA** and **PEI** in D_2O (**PEI** with pure acetic acid was used as control). The stoichiometric ratio between **NPA** and **PEI** was varied to 6.8 (**NPA-PEI-1**), 2.2 (**NPA-PEI-2**) and 1.6 (**NPA-PEI-3**), Acetonitrile (AcCN) was used to dissolve **NPA**.

13. References

1 A. Maksimenko, F. Dosio, J. Mougin, A. Ferrero, S. Wack, L. H. Reddy, A.-A. Weyn, E. Lepeltier, C. Bourgaux, B. Stella, L. Cattel and P. Couvreur, *Proc. Natl. Acad. Sci.,* 2014, **111**, E217-226.

2 L. Clima, D. Peptanariu, M. Pinteala, A. Salic and M. Barboiu, *Chem. Commun.,* 2015, **51**, 17529–17531.

3 M. Sandor, A. Riechel, I. Kaplan and E. Mathiowitz, *Biochimi. Biophys. Acta,* 2002, **1570**, 63–74.

4 S. Paliwal, M. Wales, T. Good, J. Grimsley, J. Wild and A. Simonian, *Anal. Chim. Acta,* 2007, **596**, 9–15.

5 D.-H. Kim, M. Vinoba, W.-S. Shin, K.-S. Lim, S.-K. Jeong and S.-H. Kim, *Korean J. Chem. Eng.,* 2011, **28**, 2081–2085.

6 M. Lopez, H. Vu, C. K. Wang, M. G. Wolf, G. Groenhof, A. Innocenti, C. T. Supuran and S.-A. Poulsen, *J. Am. Chem. Soc.,* 2011, **133**, 18452–18462.

7 N. P. Gabrielson and D. W. Pack, *Biomacromolecules,* 2006, **7**, 2427–2435.

8 M. L. Forrest, G. E. Meister, J. T. Koerber, and D. W. Pack, *Pharm. Res.,* 2004, **21**, 361–371.